Quantized reflection of a soliton by a vibrating atomic mirror

Wei Xiong,[1,2] Peng Gao,[3] Zhan-Ying Yang,[1,2,4,*] and Wen-Li Yang[1,2,4,5]
[1]*School of Physics, Northwest University, 710127 Xi'an, China*
[2]*Shaanxi Key Laboratory for Theoretical Physics Frontiers, 710127 Xi'an, China*
[3]*Graduate School, China Academy of Engineering Physics, 100193 Beijing, China*
[4]*Peng Huanwu Center for Fundamental Theory, 710127 Xi'an, China*
[5]*Institute of Modern Physics, Northwest University, 710127 Xi'an, China*

(Received 26 May 2023; accepted 14 July 2023; published 1 August 2023)

We numerically study the dynamics of a one-dimensional matter-wave soliton colliding with a vibrating atomic mirror. After colliding, the soliton splits into several wave packets with discrete momentum, and the kinetic energy of internal atoms is quantized. The reflected wave packets are originally diffusing but can form soliton states by quenching the nonlinear strength. The number and total kinetic energy of wave packets are obviously dependent on the vibrating amplitude and frequency of the mirror. We extend the physical system to an atomic mirror with double-frequency vibration, where the property of energy quantization also occurs and is related to the difference frequency. Our results may provide an effective way to prepare and manipulate matter-wave solitons, and are expected to contribute to the development of soliton interferometers.

DOI: 10.1103/PhysRevA.108.023303

I. INTRODUCTION

Ultracold atoms [1–3] with easy manipulation and strong coherence have been used in many research fields related to precision measurement, such as atomic frequency standards, atomic optics, and atomic interference [4–7]. A key component of bright soliton interferometers is the mechanism of coherent splitting and recombination of solitary matter waves [8–10]. Therefore, the control of matter-wave solitons is particularly important. In general, a soliton can be trapped by using a magnetic field [11,12] and optical field [13–16] in experiment. Meanwhile, a soliton can also be reflected by an atomic mirror [17], which provides another way to manipulate it effectively.

In 1982, Cook and Hill first proposed an idea of using the light field of a blue-detuned evanescent wave to reflect atomic beams [18]. When the optical field is in blue detuning, the evanescent wave optically coupled perpendicular to the surface of a medium will strongly repel atoms, so it can be used to reflect atomic beams. This kind of atomic mirror has an advantage that it has more reflectivity than an atomic mirror by a magnetic field, where cold atoms can be reflected back from the ferromagnetic surface through the stern gram effect [19]. Based on the principle of evanescent waves, many kinds of devices controlling atoms were designed theoretically, such as a new type of gradient optical trap of neutral atoms [17], a new type of atom beam splitter [20], and the silicon atom reflector [21]. In order to manipulate cold atoms more accurately, the influence of the roughness of the mirror surface on the atomic reflection has been studied [22–24]. In addition, the reflected atoms and matter-wave solitons could also manifest interesting inelastic bounce and chaotic dynamics [25,26].

Besides changing the motion of initial solitons, changing the motion of the atomic mirror can also produce distinct and interesting dynamical phenomena. In our previous work, the atomic mirror by the evanescent wave was accelerated to effectively control the uniform diffusion, shrink, and breathing of matter-wave solitons [27]. It is also noted that the diffraction of atoms happened after interacting with a vibrating atomic mirror, as shown in Colombe's work [28]. This particular dynamics and its potential application on atomic interferometers arouse our interest in reflecting dynamics of matter-wave solitons.

In this paper, we manipulate the splitting of matter-wave solitons with vibrating atomic mirrors and study the effect of vibration on soliton dynamics in different aspects. The reflected soliton splits into several diffusing wave packets, and they can be restored to soliton states after quenching the nonlinear strength. The momentum of wave packets is discrete, and the kinetic energy of atoms presents perfect quantization characteristics. The effects of vibrating amplitude and frequency of the mirror on the wave-packet dynamics are different, and when the amplitude and frequency exceed a certain limit the effect of the vibrating mirror on solitons tends to be a stationary mirror. Finally, we also study the effect of a double-frequency vibrating mirror on matter-wave solitons, and find that the greatest common divisor of frequencies plays a key role in the quantized kinetic energy, instead of intrinsic frequency.

II. PHYSICAL SYSTEM AND THE ATOMIC MIRROR

The dynamics of Bose-Einstein condensates (BECs) trapped by an external potential and interacting with an optical

*zyyang@nwu.edu.cn

potential can be described by the Gross-Pitaevskii equation (GPE) [29–31]:

$$i\hbar\frac{\partial}{\partial t}\Psi(\mathbf{r},t)=\Big[-\frac{\hbar^2}{2m}\nabla^2+V_{\rm trap}(\mathbf{r})+V_{\rm mir}(\mathbf{r},t)+g_{3D}|\Psi(\mathbf{r},t)|^2\Big]\Psi(\mathbf{r},t), \tag{1}$$

where $\mathbf{r}$ and t denote the coordinates of space and time, respectively. $\Psi(\mathbf{r},t)$ is the macroscopic wave function, and the total number of atoms is

$$n=\int_{-\infty}^{\infty}|\Psi(\mathbf{r},t)|^2d\mathbf{r}. \tag{2}$$

$V_{\rm trap}$ is an external potential confining the condensate, and $V_{\rm mir}$ is an optical dipole repulsive potential generated by the atomic mirror. The first term on the right side of Eq. (1) corresponds to kinetic energy. And the last term represents the contact interaction between atoms, whose strength is $g_{3D}=4\pi\hbar^2a_s/m$ with the atom mass m and the s-wave scattering length a_s. $a_s>0$ and $a_s<0$ indicate that the interaction between atoms is repulsive and attractive, respectively.

In our paper, we consider a BEC tightly confined in y and z directions by a harmonic potential $V_{\rm trap}=m\omega_\perp^2(y^2+z^2)/2$, and there exists an optical dipole potential $V_{\rm mir}$ only related to the x direction. Now, we employ an ansatz:

$$\Psi(\mathbf{r},t)=\psi(x,t)\psi_\perp(y,z)e^{-i\omega_\perp t}, \tag{3}$$

where $\psi_\perp(y,z)=\exp[-(y^2+z^2)/2l_\perp^2]/(l_\perp\sqrt{\pi})$ and $l_\perp=\sqrt{\hbar/m\omega_\perp}$. By multiplying both sides of the equation by $\psi_\perp^*(y,z)$ and integrating on the y and z directions, the following one-dimensional GPE can be obtained:

$$i\hbar\frac{\partial}{\partial t}\psi(x,t)=\Big[-\frac{\hbar^2}{2m}\frac{\partial^2}{\partial x^2}+V_{\rm mir}(x,t)+g_{1D}|\psi(x,t)|^2\Big]\times\psi(x,t), \tag{4}$$

where $g_{1D}=2\hbar\omega_\perp a_s$ is the strength of one-dimensional nonlinearity. In this situation, the number of atoms in Eq. (4) is still $\int_{-\infty}^{+\infty}|\psi(x,t)|^2dx=n$ due to $\iint_{-\infty}^{+\infty}|\psi_\perp(y,z)e^{-i\omega_\perp t}|^2dydz=1$ in Eq. (3). $V_{\rm mir}(x,t)$ is an exponential potential that represents the atomic mirror. When $a_s<0$ and $V_{\rm mir}(x,t)=0$, Eq. (4) supports the bright soliton solution [32]:

$$\psi(x,t)=\frac{l_\perp b}{\sqrt{-2a_s}}\,\mathrm{sech}[b(x-v_st)]e^{i(k_sx-\mu t)}, \tag{5}$$

where v_s represents the soliton's velocity, b determines its amplitude and width, $k_s=mv_s/\hbar$ is the wave number, and $\mu=\frac{\hbar}{2m}(k_s^2-b^2)$ is the chemical potential.

We refer to the experimental setup in Ref. [25] as shown in Fig. 1. The BEC is placed at the left side of the device and moves towards the right to collide with the atomic mirror. We choose the x direction as the normal direction of the mirror surface and the y-z plane as the plane of incidence. The atomic mirror is mainly composed of glass with refractive index $n=1.7$ and laser beam wavelength $\lambda=650$ nm. The evanescent wave is generated by total internal reflection at a glass surface in vacuum. The optical dipole potential for a two-level atom

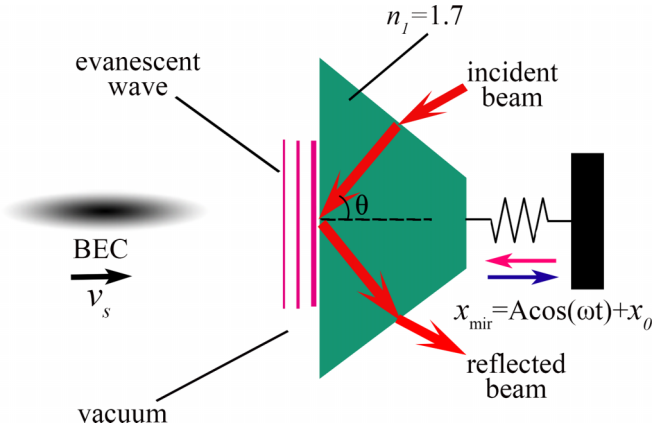

FIG. 1. A simulative experimental setup to implement the collision between the BECs and the atomic mirror. The gray ellipse on the left is the BECs. The mirror is on the right, the green trapezoid is glass, and the red arrow indicates the propagation path of the beam. The wavy line on the far right represents a spring, and the arrows below it represent the vibration direction.

can be written as

$$V_{\rm mir}=V_0\,e^{2\kappa[x-x_{\rm mir}(t)]},$$

where $x_{\rm mir}(t)$ is the position of the glass surface. We have $\kappa=k_0\sqrt{n^2\sin^2\theta-1}$ when angle of incidence $\theta=75^\circ$ is larger than the critical angle $\theta_c=\arcsin n^{-1}$. The wave number is $k_0=2\pi/\lambda$. The maximum potential at the prism surface is $V_0=\hbar\delta s_0/2$ with large laser detuning $|\delta|\gg\Gamma$ and low saturation $s_0\ll1$. $s_0=(\Gamma/2\delta)^2TI/I_0$ is the saturation parameter, where $I_0=1.65\mathrm{mW/cm^2}$ is the saturation intensity for ultracold atoms and $\Gamma=2\pi\times6.0$MHz is the natural linewidth. The intensity of the incident beam in the glass substrate is given as I, which is set as $1\,\mathrm{W/cm^2}$ and is enhanced by a factor $T=6$. $\delta=\omega_l-\omega_a$ is the detuning of the laser frequency ω_l relative to atomic resonance frequency ω_a. The evanescent wave is blue detuning when $\delta>0$, which yields an exponential repulsive potential for incident atoms, and the detuning frequency can be set as $\delta=200\,\Gamma$. Therefore, the potential of the evanescent wave is $V_{\rm mir}=9.035\times10^{-27}\mathrm{J}\times\exp\{12.6\,\mu\mathrm{m}^{-1}[x-x_{\rm mir}(t)]\}$. In our paper, an atomic mirror with simple harmonic vibration is considered. The kinematic equation of the mirror is

$$x_{\rm mir}(t)=A\cos(\omega t)+x_0, \tag{6}$$

where A, ω, and x_0 represent the vibrating amplitude, angular frequency, and equilibrium position of mirror vibration, respectively. The standard vibrating frequency f can be calculated by $f=\omega/2\pi$ to describe the mirror's vibrating times in unit time. In our paper, the regime of vibrating amplitude A and angular frequency of atomic mirror ω are 0–1 μm and 30–90 kHz, respectively.

We consider the condensates of ^{87}Rb, whose atomic mass is $m=1.445\times10^{-25}$ kg, and the transverse trapping frequency can be $\omega_\perp=2\pi\times159$ Hz. Thus, the transverse harmonic oscillator is $l_\perp=0.855\,\mu$m. If there are no special instructions, the s-wave scattering length is set as $a_s=a_{s0}$ in this paper, where $a_{s0}=-1.62a_0$ is its reference value and a_0 is Bohr radius. The adjustment of a_s can be realized by

Feshbach resonance technique [33,34]. The initial velocity of the soliton is set as $v_{s0} = 5.12\,\mathrm{mm/s}$. The set of all above parameters is in a feasible range of experiment.

III. QUANTIZED REFLECTION AND MANIPULATION OF A SOLITON

At the initial time $t = 0$, the soliton with velocity v_{s0} moves towards the mirror. According to the soliton solution (5), an initial condition can be set as

$$\psi(x,0) = \frac{l_\perp b}{\sqrt{-2a_{s0}}}\mathrm{sech}(bx)\exp(\frac{im}{\hbar}v_{s0}x), \tag{7}$$

where b is related to the width and amplitude of the soliton. To numerically simulate the dynamical process, the numerical method of solving the time-dependent nonlinear Schrödinger equation (4) is the split-step Fourier method [35]. For the initial condition (7), the parameters are set as $v_{s0} = 5.12\,\mathrm{mm/s}$, $b = 1.17\,\mu\mathrm{m}^{-1}$, $A = 0.3\,l_\perp = 0.257\,\mu\mathrm{m}$, $\omega = 50\,\mathrm{kHz}$, and $x_0 = 10.26\,\mu\mathrm{m}$, and the evolution of the whole collision process is shown in Fig. 2(a). It can be found that the soliton becomes a series of wave packets with different velocities after collision. In order to observe the collision process more clearly, the evolution plot is magnified partially in Fig. 2(b). The dipole repulsion potential generated by the evanescent wave is an exponential potential, so atoms are bounced back before touching the surface of the medium. Multiple wave packets with different velocities interfere with each other, resulting in the appearance of interference fringes. Figure 2(c) shows the density distribution of condensates at different times, where I, II, and III severally denote the first, second, and third wave packets from the right. One can find that the after-splitting wave packets are diffusing so they cannot maintain the original soliton state. (Meanwhile, in this case, we also implement numerical simulation of a three-dimensional model, whose related result and discussion can be seen in the Appendix.)

The phenomenon of soliton splitting is manifested in wave packets with different velocities, which prompts us to study the density distribution in momentum space. By the Fourier transformation of wave function $\psi(x,t)$ about x, the wave function in momentum space can be written as

$$\phi(k,t) = \frac{1}{\sqrt{2\pi}}\int_{-\infty}^{\infty}\psi(x,t)e^{-ikx}dx, \tag{8}$$

where k is the wave number to represent indirectly the momentum of condensates. When $t = 2.8\,\mathrm{ms}$, the density distribution of condensates in the momentum space is shown in Fig. 2(d). The wave packet of the dashed curve is the density distribution of the soliton in the momentum space at the initial time $t = 0$, which locates at around $k_{s0} = mv_{s0}/\hbar$ (the solid blue dotted line). The black solid curves represent the density distribution at momentum space after the collision. It can be found that the wave packets are discrete, which illustrates a regular distribution. The blue dot-dashed line is $k = k_{s0}$ and the red dashed line is $k = -k_{s0}$ in Fig. 2(d). The results indicate that the speed of some atoms remains unchanged after collision.

As shown above, the reflected wave packets will diffuse with time. Nevertheless, there are still effective ways to make

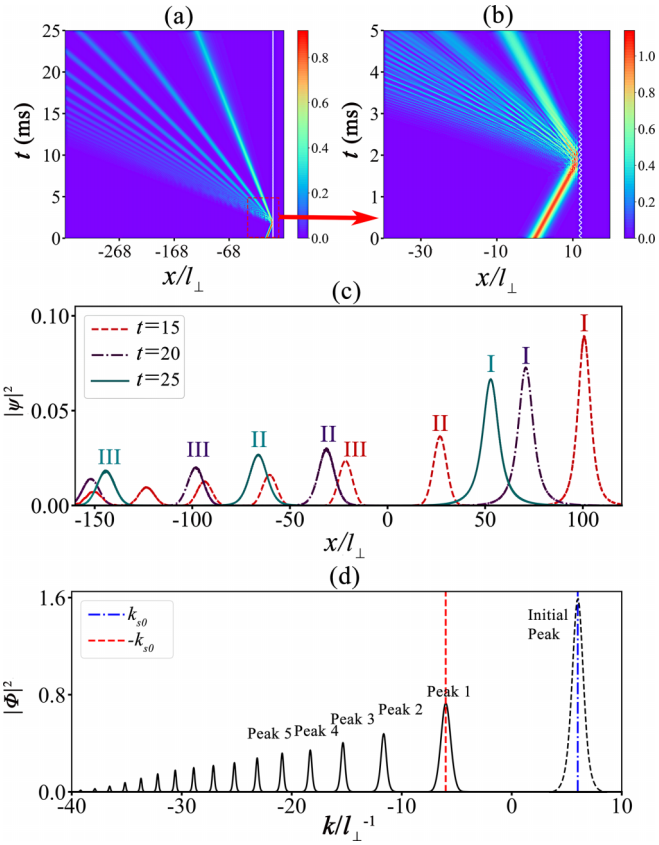

FIG. 2. (a) Density evolution plot of the collision between soliton and mirror. The initial condition is Eq. (7), and the parameters are set as $A = 0.26\,\mu\mathrm{m}$, $\omega = 50\mathrm{kHz}$, $x_0 = 10.26\,\mu\mathrm{m}$, $b = 1.17\,\mu\mathrm{m}^{-1}$, and $v_{s0} = 5.124\,\mathrm{mm/s}$. The white solid curve shows the change of mirror position with time. (b) Partially amplified plot of panel (a) in the range of $-40 < x/l_\perp < 15$ and $0 < t < 5\,\mathrm{ms}$. (c) Density distribution of wave packets after collision when $t = 15\,\mathrm{ms}$ (red dashed curve), $t = 20\,\mathrm{ms}$ (purple dot-dashed curve), and $t = 25\,\mathrm{ms}$ (green solid curve). (d) Density distribution of condensates in momentum space after collision when $t = 2.8\,\mathrm{ms}$. The black solid curve indicates the distribution of solitons in momentum space at the initial time. The blue dot-dashed and red dashed lines denote the position of $k = k_{s0}$ and $-k_{s0}$, respectively.

them remain soliton states, which have the density distribution unchanged with time. We speculate that the collision with the vibrating mirror breaks the balance between the nonlinear and dispersion effects of the initial soliton, and the attractive interaction between atoms is not enough to support wave packets to maintain stable soliton states. It prompts us to try adjusting the parameters of the BEC system or atomic mirror to restrain the diffusing phenomenon. On the one hand, we found that with some combinations of vibrating frequency and amplitude, the reflected wave packet I can still form the soliton state when $a_s = a_{s0}$. For the initial condition (7) we set the parameters $a_s = a_{s0}$, $A = 0.3\,l_\perp = 0.257\,\mu\mathrm{m}$, and $\omega = 60\,\mathrm{kHz}$, and the result is shown in Fig. 3(a), where the wave packet I remains a soliton state. Figure 3(b) shows some reflected dynamics of the soliton with different A and ω. There are three kinds of reflected wave-packet dynamics: soliton state, diffusing, and shrinking. Considering that the atom number of every

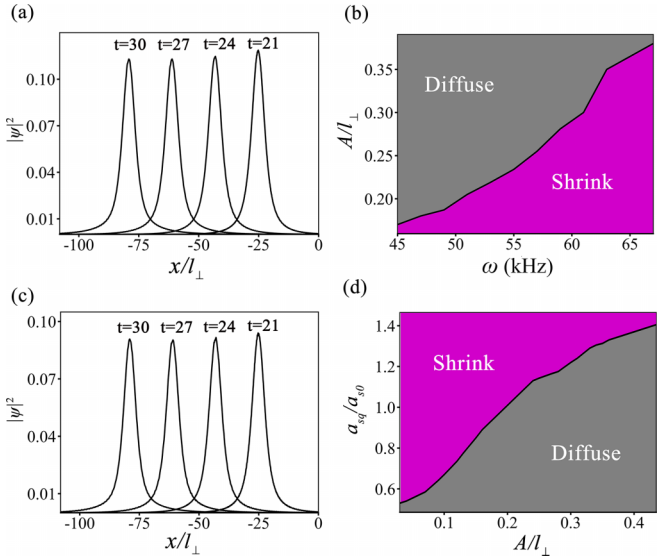

FIG. 3. (a) Density distribution of wave packet I when $t = 21$ ms (orange curve), $t = 24$ ms (green curve), $t = 27$ ms (blue curve), and $t = 30$ ms (purple curve) in the case of $a_s = a_{s0}$, $A = 0.3\,l_\perp = 0.257\,\mu$m, $\omega = 60$ kHz. (b) Reflected dynamics of a soliton with different A and ω when $a_s = a_{s0}$. The gray and red regions correspond to the diffusing and shrinking dynamics. (c) The same as panel (a) except for using quenching with $a_{sq} = 1.26a_{s0}$ and changing parameters into $A = 0.5\,l_\perp = 0.428\,\mu$m, $\omega = 80$ kHz. (d) Reflected dynamics of a soliton with different a_{sq} and ω when $a_s = a_{s0}$ and $\omega = 80$ kHz.

wave packet remains unchanged during its propagating process, we differentiate these dynamics by measuring the change of its amplitude peak value: an unchanging, decreasing, or increasing amplitude peak indicates a soliton, diffusing, or shrinking state, respectively. In Fig. 3(b), the wave packet I in the gray or red area will diffuse or shrink, and the frequency and amplitude corresponding to the black line are the special conditions for soliton formation of wave packet I. On the other hand, in experiments, the interaction strength between atoms can be controlled by Feshbach resonance, and the quenching technique can be applied to abruptly change the strength [36–40], which provides another feasible way to manipulate wave packets. We can quench the s-wave scattering length a_s, i.e., abruptly change its value after the main part of the soliton collides with the mirror. So the s-wave scattering length can be expressed as

$$a_s = \begin{cases} a_{s0}, & t < t_q \\ a_{sq}, & t \geqslant t_q, \end{cases}$$

where a_{sq} is the s-wave scattering length after quench and t_q is the time when the quench is exerted. In the case of $a_s = a_{s0}$, $A = 0.5\,l_\perp = 0.428\,\mu$m, $\omega = 80$ kHz, and $t_q = 3$ms, the wave packet I will diffuse (whose result is not shown in this paper). However, after the s-wave scattering length is changed into $a_s = 1.26\,a_{s0}$, it forms a soliton state as shown in Fig. 3(c), which indicates that the quench can induce the formation of the soliton. In Fig. 3(d), the dynamics of wave packet I under different a_s and A is illustrated when $\omega = 80$ kHz, where the diffusing, shrinking, and self-trapping states can be induced in different cases.

IV. MOMENTUM QUANTIZATION OF WAVE PACKETS

The quantized momentum distribution is another noteworthy character of reflected wave packets, as shown in Fig. 2(d). In this section, we pay attention to the effect of the mirror's vibrating frequency and amplitude on the momentum after collision. For the initial condition (7), we set $A = 0.3\,l_\perp = 0.257\,\mu$m, $\omega = 50$ kHz. The vibrating amplitude A is fixed as $0.2565\,\mu$m, and Figs. 4(a)–4(c) show the density distribution in momentum space when $t = 2.8$ ms in the cases of different vibrating frequency ω. One can find that a higher frequency can induce a smaller number of peaks and a larger distance between wave packets. We numerically calculate the particle number N_n of the nth wave packet by

$$N_n = \int_{K_n}^{K_{n+1}} |\phi_n|^2 dk, \qquad N = N_1 + N_2 + N_3 + \ldots + N_n \tag{9}$$

where ϕ_n represents the atom number density of the nth wave packet in momentum space. K_n and K_{n+1} are respectively the bottom and top limitation of the integral, which depend on the minimum point of density in different parts of momentum space. The corresponding atom number of different wave packets is marked by the red points in Fig. 4. We find that the first wave packet always has the largest number of atoms. By comparison, when the vibrating frequency is fixed as $\omega = 50$ kHz, the cases of different vibrating amplitude are shown in Figs. 4(d)–4(f). The increase of amplitude leads to the appearance of more wave packets and less atoms of the first wave packet, but the momentum interval between wave packets hardly changes.

We define the top point of the nth wave packet as its position k_n in the momentum space, and only the wave packets whose atom number density $|\phi_n(k,t)|^2 > 100\,l_\perp$ are considered. For the initial state (7), when the parameters are $A = 0.5\,l_\perp = 0.428\,\mu$m, $\omega = 80$ kHz, the relationship between n and k_n is shown in Fig. 5(a). It shows a smooth curve. Interestingly, the relationship between k_n^2 and n is almost a perfect straight line in the inset of Fig. 5(a). The equation of this line is numerically fitted by $k_n^2\,l_\perp^2 = 159.73n - 123.66$. We recall that there is no obvious relationship between the momentum coordinate of the nth wave packet and the vibrating amplitude A in Fig. 4. Thus, the momentum of the nth wave packet is only related to the vibrating frequency ω and initial velocity v_{s0}. In our paper, higher frequency $\omega > 30$ kHz and relatively lower speed $v_{s0} < \sqrt{2\hbar\omega/m}$ are considered. According to our numerical results, a higher vibrating frequency makes the quantized phenomenon more obvious, and its lowest limit is found to be around 30 kHz in the cases we are concerned with. If the vibrating frequency is too low, a vibrating mirror will be equivalent to an accelerating mirror, so the reflected dynamics caused by it will be dominated by diffusing or shrinking, instead of quantized splitting. Therefore, the condition $\omega > 30$ kHz is used in our paper. Also, the reason for using the condition of low velocity is to make all the reflected wave packets have velocity $|v| \leqslant v_{s0}$, which can simplify our study and analysis. This condition is equivalent to $\frac{1}{2}mv_{s0}^2 < \hbar\omega$. According to the numerical results of different cases, the fitting equations between k_n^2 and n indicate a relationship as follows:

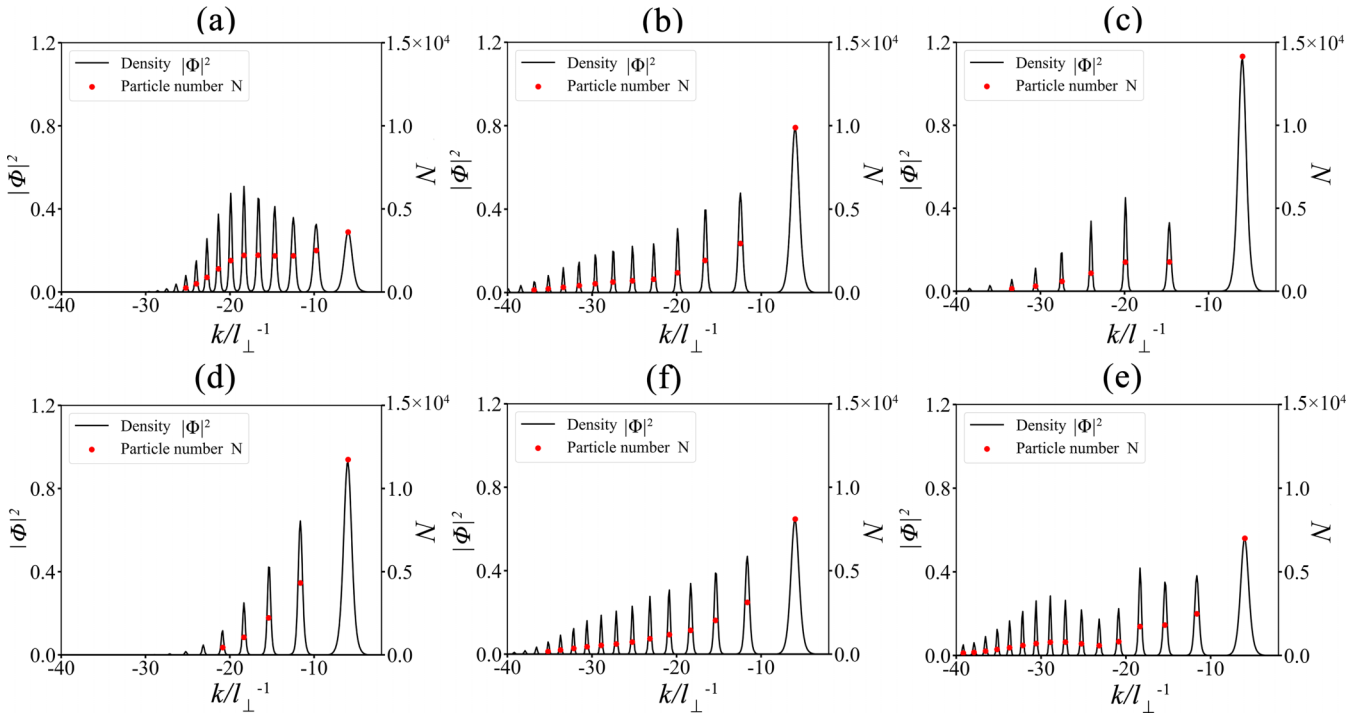

FIG. 4. Density distribution of condensates in momentum space after collision when $t = 2.8$ ms. (a–c) Results in the cases of $\omega = 30$, 60, and 90 kHz when $A = 0.3\,l_\perp = 0.257\,\mu$m. (d–f) Results in the cases of $A = 0.15\,l_\perp = 0.128\,\mu$m, $A = 0.3\,l_\perp = 0.257\,\mu$m, and $A = 0.45\,l_\perp = 0.385\,\mu$m when $\omega = 50$ kHz. The black dashed curve and red points denote the atom number density in momentum space and the corresponding atom number of wave packets, respectively. The initial condition is Eq. (7), and the other parameters are the same as those in Fig. 2(d).

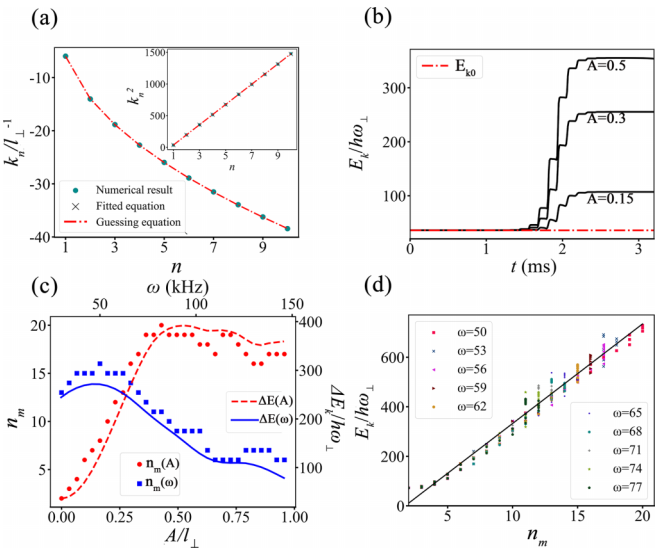

FIG. 5. (a) Change of momentum k_n of the nth wave packet. The green points, black crosses, and red dot-dashed curve denote the results of numerical simulation, numerical fitting, and Eq. (10). (b) Evolution of total kinetic energy of BECs with time when $A = 0.15\,l_\perp = 0.128\,\mu$m, $A = 0.3\,l_\perp = 0.257\,\mu$m, and $A = 0.45\,l_\perp = 0.385\,\mu$m. The red dot-dashed line denotes the initial kinetic energy E_{k0}. (c) Dependence of the wave packet's number n_m on A (red circles) and ω (blue squares). Dependence of the kinetic-energy difference ΔE_k on A (red dashed) and ω (blue solid). (d) Relationship between peak number n_m and kinetic energy ΔE_k at different frequencies ω; points represent numerical simulation results, and black lines represent equations for numerical fitting

$(k_n l_\perp)^2 = 2\omega(n-1)/\omega_\perp + (k_{s0} l_\perp)^2$. Significantly, when the expression is converted from wave-number space into velocity space, this relationship becomes

$$\tfrac{1}{2} m v_n^2 = \hbar\omega(n-1) + \tfrac{1}{2} m v_{s0}^2, \tag{10}$$

where n is an integer. v_n is the velocity of atoms in the nth wave packet while v_{s0} is the initial velocity of atoms. Thus, the difference between the initial and final kinetic energy of atoms is exactly the integer multiple of $\hbar\omega$, which equals to the energy of a photon or phonon with frequency ω.

This quantization phenomenon of the atom's kinetic energy in linear systems has been explained in different ways [20,41]. A simple interpretation can be given by analyzing the wave functions of the atom and their boundary conditions. We consider that the incident and reflected wave functions of the atom have the form of plane waves, and the mirror potential is steep enough to reflect atoms almost elastically. Before the interpretation is given, it is necessary to account for its applicable condition, i.e., $2KA\omega \ll \Omega$. The right-hand side of sign "$\ll$" denotes the inherent energy of the wave, while its left-hand side denotes the instantaneous maximal energy transferred from mirror into wave. Only when the transferred energy is far lower than the inherent energy, a perturbed plane wave can be considered as the approximative solution of the GPE. Under the condition $2KA\omega \ll \Omega$, the approximative solution can be written as

$$\begin{aligned} \psi_{\rm inc}(x,t) &= \frac{\hbar a}{\sqrt{m}} \exp[i(Kx - \Omega t)], \\ \psi_{\rm refl}(x,t) &= \frac{\hbar a}{\sqrt{m}} \exp[i(-Kx - \Omega t + \phi)], \end{aligned} \tag{11}$$

where a influences the amplitude of the wave, ϕ denotes the extra phase after the atom is reflected, and K is the initial wave number of atoms. The initial wave frequency is

$$\Omega = \Omega_L + \Omega_N = \frac{\hbar K^2}{2m} + g_{1D}\frac{\hbar a^2}{2m},$$

which contains the linear and nonlinear parts. Thus, the boundary condition at $x = x_{\rm mir}$ is

$$Kx_{\rm mir} - \Omega t + \pi = -Kx_{\rm mir} - \Omega t + \phi, \tag{12}$$

where π originates from the half-wave loss of reflection. One can find that, no matter what the nonlinear strength g_{1D} is set as, the derived extra phase is always

$$\phi = 2Kx_{\rm mir} + \pi, \tag{13}$$

so the reflected wave function is

$$\psi_{\rm refl}(x,t) = \frac{\hbar a}{\sqrt{m}}\exp[i(-Kx - \Omega t + 2Kx_{\rm mir} + \pi)]. \tag{14}$$

We recall the mirror's kinematic equation $x_{\rm mir} = A\cos(\omega t) + x_0$ and apply the Fourier series expansion on $\psi_{\rm refl}(x,t)$. The reflected wave function can be expressed as

$$\psi_{\rm refl}(x,t) = -\frac{\hbar a}{\sqrt{m}}e^{-iK(x-2x_0)}\sum_{n=-\infty}^{+\infty} i^n J_n(2KA) \times \exp[-i(\Omega - n\omega)t], \tag{15}$$

where n is an integer and $J_n(z)$ is the first kind of Bessel function. One can find that the difference between the initial and final kinetic energy of atoms is

$$\hbar\Delta\Omega = -n\hbar\omega,$$

which is the quantization of kinetic energy of reflected atoms. This result is equivalent to Eq. (10) except for the trivial difference of n values. Meanwhile, it indicates the kinetic-energy levels of atoms are not influenced by the nonlinear strength g_{1D}, so it provides a possible way to understand the reason why the nonlinear term in the GPE has no effect. Although the above analysis is not rigorous enough to some extent, it provides a simple way to understand well the quantized result of the atom's kinetic energy.

When the frequency $\omega = 50\,\text{kHz}$ is fixed, we set $A = 0.15\,l_\perp = 0.128\,\mu\text{m}$, $A = 0.3\,l_\perp = 0.257\,\mu\text{m}$, and $A = 0.45\,l_\perp = 0.385\,\mu\text{m}$, and the evolution of kinetic energy is shown in Fig. 5(b). The kinetic energy of BECs rapidly increases when it collides with the mirror. The results above show that the amplitude A and frequency ω of the mirror have a significant impact on the number n_m of wave packets after collision. Thus, the dependence of n_m on ω and A is investigated in the Fig. 5(c) point graph. The parameter is set as A ranging from zero to $l_\perp$, and ω ranging from 30 to 150 kHz. It is found that the number of wave packets always decreases with the increase of vibrating frequency ω, but first increases and then slightly decreases with the increase of vibrating amplitude A. Meanwhile, it is known that the total kinetic energy E_k of condensates will increase after colliding with the mirror, whose value can be calculated by the integral of $|\partial\psi/\partial x|^2/2$ in the whole range of x. Its difference before and after collision is defined by $\Delta E_k = E_k - E_{k0}$.

The dependence of ΔE_k on A and ω is shown in the Fig. 5(c) curve graph. The red dot-dashed line is the kinetic energy at the initial time, the other three curves correspond to different A, and the "steps" denoting ΔE_k are caused by the interaction with the mirror. ΔE_k first increases and then slightly decreases with A increasing; ΔE_k always decreases with ω increasing. In addition, with the very high ω or small A, both the number of wave packets and kinetic-energy difference are very close to their minimal values, which is similar to the result of the stationary mirror. Interestingly, these results of ΔE_k and n_m shown in Fig. 5(c) are very similar, which indicates that A and ω have a similar influence on ΔE_k and n_m. Therefore, we further explore the relationship between n_m and ΔE_k. As shown in Fig. 5(d), dots with different colors represent the relationship between n_m and ΔE_k with different ω and A, and there is an approximatively linear relation as expected. The numerical fitting gives the linear function between them, i.e., $E_k/\hbar\omega = 40.21n_m - 69.73$, which is denoted by the black line in Fig. 5(d).

V. VIBRATING ATOMIC MIRROR WITH DOUBLE FREQUENCY

In this section, the double-frequency vibrating mirror is considered, whose motion is described by the following equation:

$$x_{\rm mir2}(t) = A\cos(\omega_1 t) + A\cos(\omega_2 t) + x_0. \tag{16}$$

We define the first term $A\cos(\omega_1 t) = x_1$ and the second term $A\cos(\omega_2 t) = x_2$. The change of $x_{\rm mir}$, x_1, and x_2 is shown in Fig. 6(a), which manifests a modulated periodicity. For the initial state (7), when the parameters are $A = 0.3\,l_\perp = 0.257\,\mu\text{m}$, $\omega_1 = 100\,\text{kHz}$, $\omega_2 = 150\,\text{kHz}$, $v_{s0} = 5.12\,\text{mm/s}$, and $x_0 = 10.26\,\mu\text{m}$, the evolution result is shown in Fig. 6(b). Similar to the results of a single frequency, the soliton splits into several wave packets after colliding with mirror. The distribution of atom number density in momentum space is also discrete as shown in Fig. 6(c). Meanwhile, we also pay attention to whether Eq. (10) is satisfied in this way of vibration. The equation about k_n and n we fit in the numerical simulation is $k_n^2 l_\perp^2 = 99.92n - 64.09$. Both of the results of numerical fitting and measurement are shown in Fig. 6(d), which still illustrate a linear relationship.

Based on numerical results in many cases with different ω_1 and ω_2, an exact expression can be written as

$$\tfrac{1}{2}mv_n^2 = \hbar\omega_g(n-1) + \tfrac{1}{2}mv_{s0}^2, \tag{17}$$

where $\omega_g = \text{gca}(\omega_1, \omega_2)$ is the greatest common divisor of ω_1 and ω_2. Considering that the values of ω_1 and ω_2 cannot be ideal integers in real cases, the above relation allows small fluctuation of their values to produce the most obvious quantized phenomena. However, the above relation requires that the time interval while the soliton is interacting with the mirror is greater than the modulated period of the mirror's vibration, namely $\frac{2\pi}{bv_{s0}} > \frac{2\pi}{|\omega_1-\omega_2|}$, which indicates that the frequency difference of vibration cannot be too small, namely $|\omega_1 - \omega_2| > bv_{s0}$. The relation (17) can still be explained by the approximative solution of the wave function. Substituting $x_{\rm mir2}$ into $x_{\rm mir}$ in Eq. (14), the reflected wave function after

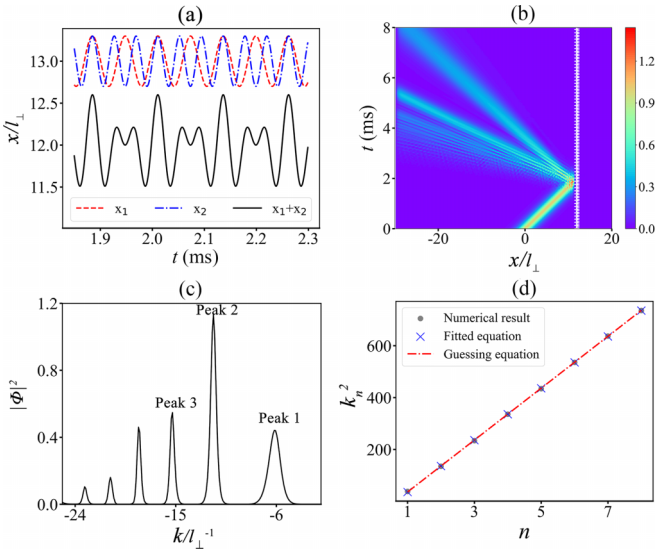

FIG. 6. (a) Position change of mirror with double-frequency vibration with time [see Eq. (16)], which is denoted by the black solid curve. The red dashed and blue dot-dashed curves are the corresponding position in the cases of single frequency. (b) Density evolution of condensates colliding with a double-frequency vibrating mirror. (c) Density distribution in momentum space when $t = 3.5$ ms. (d) Change of momentum k_n of the nth wave packet, where the unit of k_n is $l_\perp^{-1}$. The gray points, blue crosses, and red dot-dashed curve denote the results of numerical simulation, numerical fitting, and Eq. (17). The other parameters are set as $\omega_1 = 100$ kHz, $\omega_2 = 150$ kHz, $A = 0.3\, l_\perp = 0.257$ μm, and $x_0 = 10.26$ μm.

Fourier series expansion is

$$\psi_{\text{refl}}(x,t) = -\frac{\hbar a}{\sqrt{m}} e^{-iK(x-2x_0)} \sum_{n_1=-\infty}^{+\infty} \sum_{n_2=-\infty}^{+\infty} i^{n_1+n_2} \times J_{n_1}(2KA) J_{n_2}(2KA) \exp[-i(\Omega - n_1\omega_1 - n_2\omega_2)t],$$

where n_1 and n_2 are arbitrary integers. So the difference of kinetic energy becomes

$$\hbar\Delta\Omega = -\hbar(n_1\omega_1 + n_2\omega_2).$$

It is assumed that $\omega_1 = m_1\omega_g$ and $\omega_2 = m_2\omega_g$, where m_1 and m_2 are integers decided by the motion equation of the mirror. Then, the final energy of the atom is

$$\hbar\Delta\Omega = -\hbar(n_1 m_1 + n_2 m_2)\omega_g.$$

With arbitrary values of n_1 and n_2, the coefficient $n_1m_1 + n_2m_2$ can also be an arbitrary integer, which means the appearance of quantized kinetic energy with minimal interval $\hbar\omega_g$, showing a good agreement with numerical results. Meanwhile, the relation (17) is also applicable in the case of single-frequency vibration (assuming $\omega_1 = \omega_2 = \omega$), because the greatest common divisor of ω and ω is itself, so the energy interval is $\hbar\omega_g = \hbar\omega$, which agrees well with the analysis in Sec. IV.

VI. CONCLUSION

In summary, we investigate the collision between a matter-wave soliton and a vibrating atomic mirror in a one-dimensional system of BECs. The soliton will split into many wave packets after colliding with a vibrating mirror, whose character of splitting depends on the mirror's vibrating frequency and amplitude. Importantly, these wave packets can form solitons again, so they provide a way to generate matter-wave solitons, which can also be implemented by quenching the nonlinear strength shortly after collision. Meanwhile, the momentum of condensates after collision is discrete, and the kinetic energy of atoms is quantized. The change of kinetic energy before and after collision is exactly the integer times a photon's (or phonon's) energy with the same frequency as the mirror's vibration. The number of wave packets after splitting and the difference of total kinetic energy of BECs before and after collision are heavily dependent on the amplitude and frequency of vibration, and interestingly they have similar change when the amplitude and frequency are adjusted. With the vibrating amplitude decreasing or the frequency increasing, the two quantities get lower and lower. It indicates that the small amplitude or high frequency could make the vibrating mirror into a stationary one. Finally, we extend the treatment to systems of a double-frequency vibrating mirror. In some cases, the momentum distribution of condensates is still discrete, indicating the quantized atom's kinetic energy, and the numerical result demonstrates that the difference frequency is more important than the mirror's intrinsic frequency, in the transfer of the atom's kinetic energy.

Our paper provides a possible way to control matter-wave solitons and effectively divide the BECs into several small groups. The wave properties of matter-wave solitons are demonstrated from a perspective of energy quantization. It is also expected to deepen our understanding on the formation mechanism and dynamics of solitons and help in the design of soliton interferometers.

ACKNOWLEDGMENTS

The authors thank Prof. J. Liu for his helpful discussions. This work was supported by National Natural Science Foundation of China (Grants No. 12275213 and No. 11875220).

APPENDIX: THREE-DIMENSIONAL NUMERICAL SIMULATION

Considering that all of the results shown above are based on the one-dimensional GPE, we turn our attention to the three-dimensional model, which is closer to a real system of condensates and enables us to study the transverse effect. Using the same parameters as Fig. 2, the three-dimensional GPE (1) is simulated numerically and the result is shown in Fig. 7. One can see that the distinct quantized phenomenon occurs and no transverse excitation appears, after the ball of BECs is reflected by the atomic mirror. It indicates that the transverse frequency used in our paper is applicable for trapping BECs, and the dimensionality hardly has an effect on the quantized phenomenon.

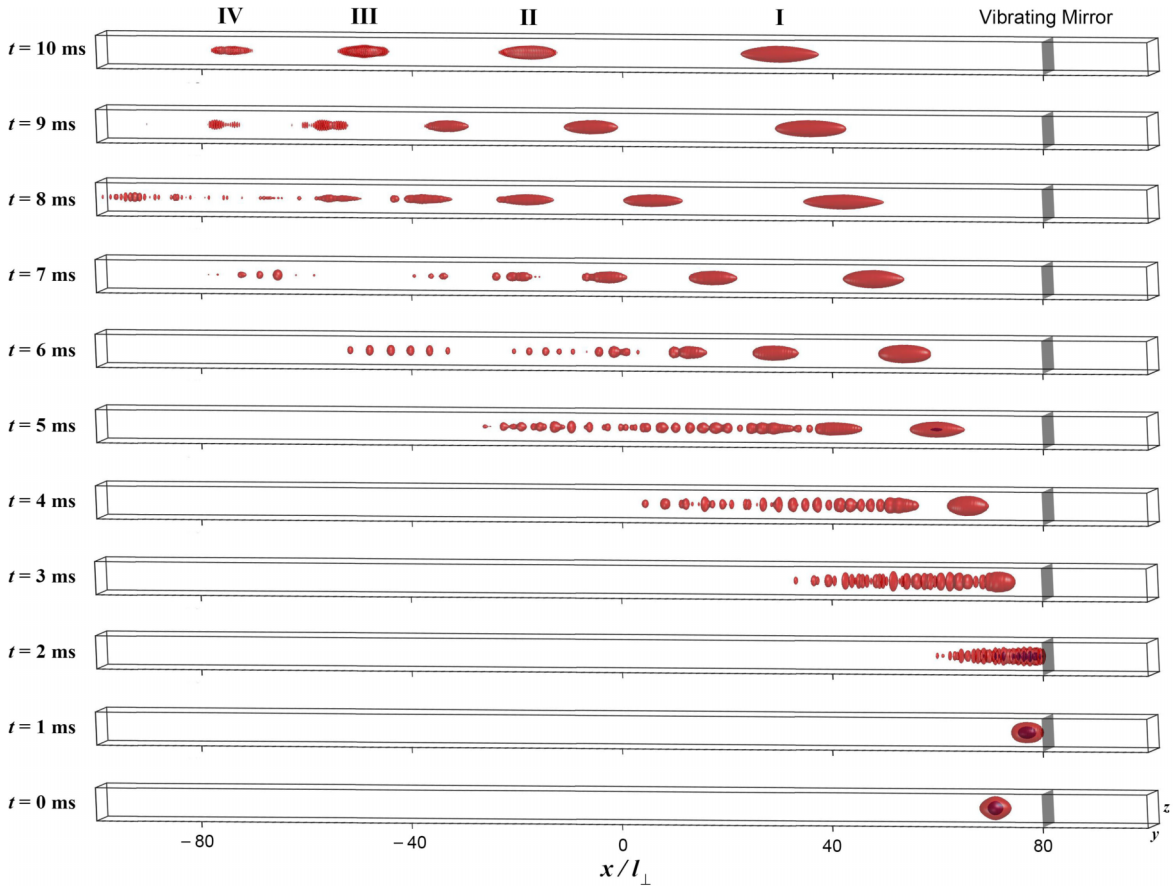

FIG. 7. Three-dimensional evolution of BEC density at times from $t = 0$ to 10 ms (from bottom to top of the plot). The external red and inner purple curved surfaces denote the density 25.5 and 509.8 μm^{-3}, respectively. The gray board denotes the position of the vibrating atomic mirror. At $t = 10$ ms, the quantized phenomenon can be observed clearly, and the BECs' density peaks are marked by I, II, III, and IV

[1] M. H. Anderson, J. R. Ensher, M. R. Matthews, C. E. Wieman, and E. A. Cornell, Observation of Bose-Einstein condensation in a dilute atomic vapor, Science **269**, 198 (1995).

[2] K. B. Davis, M.-O. Mewes, M. R. Andrews, N. J. van Druten, D. S. Durfee, D. M. Kurn, and W. Ketterle, Bose-Einstein Condensation in a Gas of Sodium Atoms, Phys. Rev. Lett. **75**, 3969 (1995).

[3] C. C. Bradley, C. A. Sackett, and R. G. Hulet, Bose-Einstein Condensation of Lithium: Observation of Limited Condensate Number, Phys. Rev. Lett. **78**, 985 (1997).

[4] F. Riehle, Th. Kisters, A. Witte, J. Helmcke, and Ch. J. Bordé, Optical Ramsey Spectroscopy in a Rotating Frame: Sagnac Effect in a Matter-Wave Interferometer, Phys. Rev. Lett. **67**, 177 (1991).

[5] M. Kasevich and S. Chu, Atomic Interferometry Using Stimulated Raman Transitions, Phys. Rev. Lett. **67**, 181 (1991).

[6] D. S. Durfee, Y. K. Shaham, and M. A. Kasevich, Long-Term Stability of an Area-Reversible Atom-Interferometer Sagnac Gyroscope, Phys. Rev. Lett. **97**, 240801 (2006).

[7] J. B. Fixler, G. T. Foster, J. M. Mcguirk, and M. A. Kasevich, Atom interferometer measurement of the newtonian constant of gravity, Science **315**, 74 (2007).

[8] J. Polo and V. Ahufinger, Soliton-based matter-wave interferometer, Phys. Rev. A **88**, 053628 (2013).

[9] G. D. McDonald, C. C. N. Kuhn, K. S. Hardman, S. Bennetts, P. J. Everitt, P. A. Altin, J. E. Debs, J. D. Close, and N. P. Robins, Bright Solitonic Matter-Wave Interferometer, Phys. Rev. Lett. **113**, 013002 (2014).

[10] J. L. Helm, S. L. Cornish, and S. A. Gardiner, Sagnac Interferometry Using Bright Matter-Wave Solitons, Phys. Rev. Lett. **114**, 134101 (2015).

[11] E. A. Cornell and C. E. Wieman, Nobel Lecture: Bose-Einstein condensation in a dilute gas, the first 70 years and some recent experiments, Rev. Mod. Phys. **74**, 875 (2002).

[12] X.-F. Zhang, Qin Yang, J.-F. Zhang, X. Z. Chen, and W. M. Liu, Controlling soliton interactions in Bose-Einstein condensates by synchronizing the Feshbach resonance and harmonic trap, Phys. Rev. A **77**, 023613 (2008).

[13] L. Fallani, F. S. Cataliotti, J. Catani, C. Fort, M. Modugno, M. Zawada, and M. Inguscio, Optically Induced Lensing Effect on a Bose-Einstein Condensate Expanding in a Moving Lattice, Phys. Rev. Lett. **91**, 240405 (2003).

[14] P. G. Kevrekidis, D. J. Frantzeskakis, B. A. Malomed, G. Herring, and A. R. Bishop, Statics, dynamics, and

manipulations of bright matter-wave solitons in optical lattices, Phys. Rev. A **71**, 023614 (2005).

[15] D. Mihalache, D. Mazilu, F. Lederer, B. A. Malomed, Y. V. Kartashov, L. C. Crasovan, and L. Torner, Stable Spatiotemporal Solitons in Bessel Optical Lattices, Phys. Rev. Lett. **95**, 023902 (2005).

[16] Y. V. Kartashov, V. A. Vysloukh, and L. Torner, Soliton shape and mobility control in optical lattices, Prog. Opt. **52**, 63 (2007).

[17] Y. B. Ovchinnikov, S. V. Shulga and V. I. Balykin, An atomic trap based on evanescent light waves, J. Phys. B **24**, 3173 (1991).

[18] R. J. Cook, R. K. Hill, An electromagnetic mirror for neutral atoms, Opt. Commun. **43**, 258 (1982).

[19] T. M. Roach, H. Abele, M. G. Boshier, H. L. Grossman, K. P. Zetie, and E. A. Hinds, Realization of a Magnetic Mirror for Cold Atoms, Phys. Rev. Lett. **75**, 629 (1995).

[20] C. Henkel, A. M. Steane, R. Kaiser and J. Dalibard, A modulated mirror for atomic interferometry, J. Phys. II (France) **4**, 1877 (1994).

[21] S. Shimizu, T. Iwane, A. Kunieda, H. Kumagai, K. Midorikawa, and M. Obara, Design of atomic mirror for silicon atoms, Sci. Technol. Adv. Mater. **5**, 581 (2004).

[22] C. Henkel, K. Molmer, R. Kaiser, N. Vansteenkiste, C. I. Westbrook, and A. Aspect, Diffuse atomic reflection at a rough mirror, Phys. Rev. A **55**, 1160 (1997).

[23] V. Savalli, D. Stevens, J. Esteve, P. D. Featonby, V. Josse, N. Westbrook, C. I. Westbrook, and A. Aspect, Specular Reflection of Matter Waves from a Rough Mirror, Phys. Rev. Lett. **88**, 250404 (2002).

[24] H. Perrin, Y. Colombel, B. Mercierl, V. Lorent and C. Henkel, Diffuse reflection of a Bose-Einstein condensate from a rough evanescent wave mirror, J. Phys. B **39**, 4649 (2006).

[25] D. Voigt, B. T. Wolschrijn, R. Jansen, N. Bhattacharya, R. J. C. Spreeuw, and H. B. van Linden van den Heuvell, Observation of radiation pressure exerted by evanescent waves, Phys. Rev. A **61**, 063412 (2000).

[26] K. P. Khamrakulov, Regular and chaotic dynamics of a matter-wave soliton near the atomic mirror, Int. J. Mod. Phys. B **28**, 1450198 (2014).

[27] W. Xiong, P. Gao, Z. Y. Yang, and W. L. Yang, Control of matter-wave solitons using an accelerating atomic mirror, J. Phys. B **55**, 145301 (2022).

[28] Y. Colombe, B. Mercier, H. Perrin, and V. Lorent, Diffraction of a Bose-Einstein condensate in the time domain, Phys. Rev. A **72**, 061601(R) (2005).

[29] C. Pethick and H. Smith, *Bose-Einstein Condensation in Dilute Gases* (Cambridge University, Cambridge, England, 2002).

[30] Y. Castin and R. Dum, Low-temperature Bose-Einstein condensates in time-dependent traps, Phys. Rev. A **57**, 3008 (1998).

[31] S. A. Gardiner and S. A. Morgan, Number-conserving approach to a minimal self-consistent treatment of condensate and non-condensate dynamics in a degenerate Bose gas, Phys. Rev. A **75**, 043621 (2007).

[32] A. Shabat and V. Zakharov, Exact theory of two-dimensional self-focusing and one-dimensional self-modulation of waves in nonlinear media, Sov. Phys. JETP **34**, 62 (1972).

[33] L. Khaykovich, F. Schreck, G. Ferrari, T. Bourdel, J. Cubizolles, L. D. Carr, Y. Castin, and C. Salomon, Formation of a matter-wave bright soliton, Science **296**, 1290 (2002).

[34] T. Volz, S. Dürr, S. Ernst, A. Marte, and G. Rempe, Characterization of elastic scattering near a Feshbach resonance in 87 Rb, Phys. Rev. A **68**, 010702(R) (2003).

[35] J. Yang, *Nonlinear Waves in Integrable and Nonintegrable Systems* (SIAM, Philadelphia, 2010).

[36] T. Kinoshita, T. Wenger, and D. S. Weiss, A quantum Newton's cradle, Nature (London) **440**, 900 (2006).

[37] E. Haller, M. Gustavsson, M. J. Mark, J. G. Danzl, R. Hart, G. Pupillo, and H.-C. Nagerl, Realization of an excited, strongly correlated quantum gas phase, Science **325**, 1224 (2009).

[38] M. Gring, O. Mandel, T. W. Hansch, and I. Bloch, Relaxation and Pre-thermalization in an Isolated Quantum System, Science **337**, 1318 (2012).

[39] A. Di Carli, C. D. Colquhoun, Grant Henderson, Stuart Flannigan, G.-L. Oppo, Andrew J. Daley, S. Kuhr, and Elmar Haller, Excitation Modes of Bright Matter-Wave Solitons, Phys. Rev. Lett. **123**, 123602 (2019)

[40] C. A. Chen and C. L. Hung, Observation of Universal Quench Dynamics and Townes Soliton Formation from Modulational Instability in Two-Dimensional Bose Gases, Phys. Rev. Lett. **125**, 250401 (2020).

[41] J. Felber, R. Gähler, and C. Rausch, Matter waves at a vibrating surface: Transition from quantum-mechanical to classical behavior, Phys. Rev. A **53**, 319 (1996).